PROC. OF JSCE
No. 300, August 1980

LOAD CARRYING CAPACITY OF TWO HINGED STEEL ARCH BRIDGES WITH STIFFENING DECK

By Shigeru KURANISHI, Tsuneaki SATO** and Mitsugu OTSUKI****

1. INTRODUCTION

Recently, a remarkable progress has been made in the field of the ultimate strength study of steel arches. Knowledge[1)~7)] of the behavior of various types of steel arches in the ultimate state considering yielding of material, finite deformations and influence of the residual stresses has been accumulated ready for practical use. A certain number of papers[3),7)] are discussing the design method of them reflecting the results obtained by the ultimate strength analysis. But, as for stiffened arches of deck type, the study is not sufficiently deepened and there are some problems left unresolved.

The in-plane collapse of stiffened arches may be differentiated in two modes. One is the failure as an integrated structure composed of an arch rib and a stiffening girder. The character of the integrated strength of stiffened arches is estimated to be similar to that of not stiffened arches. This submits a problem how to express the ultimate strength referring to that of two hinged arches. Zui, Shinke and Namita[6)] present the strength as a function of a total slenderness ratio given by using the total moment of inertia and total area of the arch rib and stiffening girder.

Another collapse is caused by the failure of arch rib members between adjacent panel points. Concerning this problem, there is no ultimate strength study reported hitherto. Especially, when the arch rib has comparatively high rigidity, the arch rib is usually designed as a continuously curved one conforming with the continuously curved arch axis. Therefore, the arch rib members between the vertical posts are regarded as initially crooked beam-columns subjected to both bending and axial compression. This large crookedness and combined stresses will reduce the strength to a certain extent compared with ordinary straight columns or beam columns. But, this reduction of the strength of the arch ribs is expected to be fairly improved by employing a polygonal arch axis which forms a straight line between the panel points of the arch.

This paper presents an approach to the above mentioned problems through parametric numerical analyses of the load carrying capacity of stiffened steel arches of deck type. The through type of stiffened arches is not referred herein considering the well-known extremely high buckling strength as a whole structure. But, as for the local failure of the arch ribs, the results presented here may be applicable to them.

In this analysis, the effect of the finite deformation, yielding of material and residual stresses is included, but the yielding and buckling of the posts is neglected.

2. METHOD OF ANALYSIS

(1) Analytical Method

The ultimate strength analysis employed herein is carried by combined use of the load incremental method and iterative method which are basically same as used in Ref. 8).

Influence of the spread of yielding of material in the longitudinal direction and cross sections, unloading from the yielded state, finite deformations of members and the residual stresses by welding on the strength is taken into account in the finite element analysis. The post members are supposed to be connected to the arch rib and stiffening girder by hinges and the stiffness matrices of the posts are formed by the first order elastic theory. But, in the iterative approach of the unbalance internal forces, the effect of the displacement of the posts is included. The Cholesky method is adopted in the calculation.

* Member of JSCE Prof., Dept. of Civil Engineering Tohoku Univ.
** Member of JSCE M. Eng., Engr. Chiba Prefecture (former graduate student of Tohoku Univ.)
*** Member of JSCE M. Eng., Engr. Kubota Ltd. (former graduate student of Tohoku Univ.)

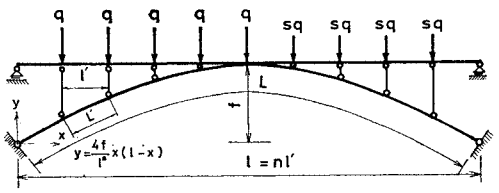

Fig. 1 Configuration of stiffened arch and loading.

(2) Numerical Model and Parameters

Stiffened arches analysed here have a parabolic solid arch rib with box cross section and a straight stiffening girder with I cross section referring to conventional configuration of stiffened steel arches. The loads and configuration of an arch are illustrated in **Fig. 1**. The arch rib and stiffening girder are connected by hinge-ended vertical posts except at the crown where they are connected rigidly as shown in **Fig. 1**. The form of the arch member between the posts are classified in three types. The first is adopted as standard one and has a continuously curved member axis which coincides with the parabolic line, the second has a straight axis and the third has a slightly crooked straight axis of which the half sinusoidal initial crookedness is one thousandth of the panel length at the middle point. Number of the panels is 10, but, in some cases, the type of 8 panels is taken up to study the influence of the panel length. The span of every stiffened arch is 100 m long and the rise is 15.0 m high except in some cases in which it is taken to 12.5 m or 20.0 m to study the influence of the rise-span ratio on the ultimate strength. To exclude the effect of deformation of the posts, the area of the posts is selected to ten times larger than the value which will be required for equilibrium with the maximum arch rib force.

Namely, the area is given by

$$A_P=\frac{80fl'}{l^2}A_A \qquad \cdots\cdots(1)$$

where A_P and A_A are the area of a post and an arch rib, respectively, l' is panel length and f is rise of an arch.

To know the effect of stiffening, the analysis is carried out by varying the flexural rigidity of the stiffening girder. The slenderness ratio λ_A of basic arch ribs to be stiffened, which is given by the ratio of the whole length L of the arch axis to the radius of gyration of the cross section, is chosen to be 198, 248, 297, 446, and 595. The proportion of a cross section of stiffened arches and stiffening girders is shown in **Fig. 2**. The total slenderness ratio is defined here by

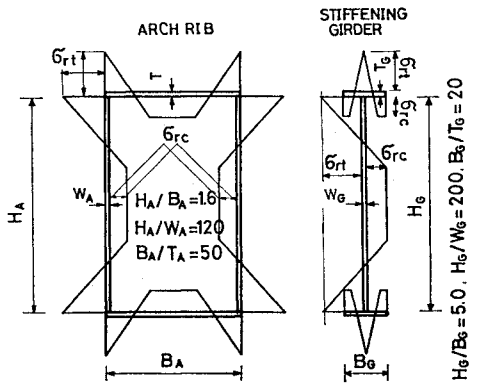

Fig. 2 Proportions of cross sections and assumed distribution pattern of residual stresses.

$$\lambda_T=\frac{L}{\sqrt{(I_A+I_G)/A_A}} \qquad \cdots\cdots(2)$$

in which, I_A=moment of inertia of an arch rib, I_G=moment of inertia of a stiffening girder and L=the whole length of the arch rib. The slenderness ratio of an arch is given by $\lambda_A=L/\sqrt{I_A/A_A}$. The total slenderness ratio is varied in this analysis from 100 to 400 approximately. The dimensions of the cross sections are determined as shown in **Table 1**, so as to realize the above mentioned range of the parameters.

The arch rib and stiffening girder are made of the same structural steel of which the yield point is 3200 kg/cm² (314 N/mm²).

When the residual stresses by welding are considered, their distribution patterns are assumed as shown in **Fig. 2** and the maximum residual stress in compression is taken as 40% of the yield point of material by refering the results of Ref. 8). In the numerical analysis, cross sections of an arch rib and stiffening girder are divided into 36 elements and 27 elements, respectively, as shown in **Fig. 3**. Number of member elements between the vertical posts is determined to be 5 judging from the result of preliminary calculation.

Two modes of loading pattern are adopted here, namely, one is unsymmetrical and another is nearly symmetrical. They are obtained by taking the loading parameter $s=0.5$ and $s=0.99$ respectively as shown in **Fig. 1**. All loads are placed on the panel points of the stiffening girder.

The ultimate strength and slenderness ratio are expressed in non-dimensional forms. The maximum value of the load is given by the ratio to the intensity of equally placed concentrated loads which produce full plastic axial force at the springings by the first order elastic analysis. Namely the load intensity q_Y is given by

Table 1 Dimensions of cross sections.

$\lambda_A/\bar{\lambda}_A$	λ_T	$\bar{\lambda}_T$	A_A (cm²)	I_A (×10⁶cm⁴)	A_G (cm²)	I_G (×10⁶cm⁴)	H_G (cm)	H_G/H_A
198/1.19	119	0.71	550	1.565	392	2.732	208.8	1.6
	139	0.83			300	1.602	182.7	1.4
	159	0.95			221	0.865	156.6	1.2
	170	1.02			179	0.562	141.0	1.1
	188	1.13			98.1	0.171	104.4	0.8
248/1.49	127	0.76	352	0.641	318	1.793	187.9	1.8
	149	0.89			251	1.119	167.1	1.6
	162	0.97			221	0.865	156.6	1.5
	180	1.08			179	0.567	141.0	1.35
	220	1.32			981	0.171	104.4	1.0
297/1.78	110	0.66	244	0.309	330	1.929	191.4	2.2
	130	0.78			273	1.318	174.0	2.0
	141	0.84			246	1.073	165.3	1.9
	153	0.92			221	0.865	156.6	1.8
	173	1.04			185	0.607	143.4	1.65
	209	1.25			136	0.316	121.8	1.4
	264	1.58			68.1	0.0823	87.0	1.0
446/2.67	94	0.56	109	0.0611	273	1.318	174.0	3.0
	123	0.74			205	0.743	150.8	2.6
	153	0.92			160	0.455	133.4	2.3
	194	1.16			121	0.260	116.0	2.0
595/3.56	143	0.86	61.1	0.0193	134	0.316	121.8	2.8
	153	0.72			124	0.274	117.5	2.7
	190	1.14			98.1	0.171	104.4	2.4
	259	1.53			68.1	0.0824	87.0	2.0

$f/l=0.15$, $l=100$ m

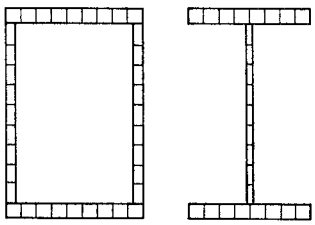

Fig. 3 Cross sectional segments.

$$q_Y=\frac{A\sigma_Y}{\sqrt{\left(\frac{n-1}{2}\right)^2+\left\{\sum_{i=2}^{n}\frac{Sl_1l_2}{8f/l}(l_1^2+3l_1l_2+l_2^2)\right\}^2}} \quad \cdots\cdots(3)$$

in which i=order number of panel point from left, n=total number of panels, $l_1=(i-1)/n$ and $l_2=1-(i-1)/n$.

The slenderness parameter is calculated by being based on the buckling formula for two-hinged arches given by Stüssi[9] as follows:

$$H_K=\alpha_K\frac{EI_A}{l^2} \quad \cdots\cdots(4)$$

in which H_K is a critical horizontal thrust and α_K is the buckling coefficient. From the above equation, the critical axial force at the springing is given as follows:

$$N_K=\frac{\alpha_K}{\cos\gamma}\frac{EI_A}{l^2} \quad \text{or} \quad N_K=\frac{S^2\alpha_K}{\cos\gamma}\frac{EI_A}{L^2} \quad \cdots\cdots(5)$$

in which γ is the inclimation angle of the arch axis at the springing and S is the ratio of L to 1. Thus, the total slenderness parameter $\bar{\lambda}_T$ is given by

$$\bar{\lambda}_T=\frac{\lambda_T}{\sqrt{\alpha_K ES^2/\sigma_Y\cos\gamma}} \quad \cdots\cdots(6)$$

The slenderness ratio which corresponds to $\bar{\lambda}_T=1$ is 165, 167 and 168 for $f/l=0.125$, 0.150 and 0.20, respectivley.

(3) Assumptions

Other major assumptions which are not explained in the previous sections are as follows:

1. Arch rib and stiffening girder have constant cross section over whole length.
2. Material of arch ribs and stiffening girders is same in grade and shows the ideal elastic-plastic stress-strain relationship and no strain hardening is considered.
3. Cross sections keep the original plane unchanged after deformation.
4. All displacements of stiffened arch are confined in the vertical plane which contains the loads and arch.
5. Loads do not change their direction after

displacements of the stiffened arch.

6. The maximum tensile residual stress σ_{rt} equals the yield point and the maximum compressive residual stress σ_{rc} is 0.4 σ_Y.
7. No local buckling of plates of members occurs.

3. NUMERICAL RESULTS

(1) Behavior for Unsymmetrical Loading

In usual case, co-operation of the flexural rigidities of arch rib and stiffening girder is expected owing to action of posts which work to enforce nearly the same vertical displacements on the arch rib and stiffening girder. **Fig. 4** shows the displacements of an arch rib and stiffening girder just before the ultimate state for the loading pattern $s=0.5$. The difference between the displacements of the arch rib and stiffening girder is so small that it can not be seen in the figures. The bending moment diagrams for the same loading are shown in **Fig. 5**. The bending moment diagrams of the arch rib members show undulation between the panel points affected by the curvature of their member axis. Especially, when the total slenderness ratio becomes smaller, this undulation becomes more significant. If straight arch rib members between the adjacent panel points are adopted, as a matter of course, this undulation becomes very small. However, the influence of the local behavior of arch rib members does not affect the ultimate strength for unsymmetrical loading of stiffened arches. **Fig. 6** shows the relationship between the load carrying capacity and the total slenderness parameter. The load carrying capacity of stiffened arches expressed in relation to the total slenderness parameter keeps a good correspondence with that of two hinged asches. However,

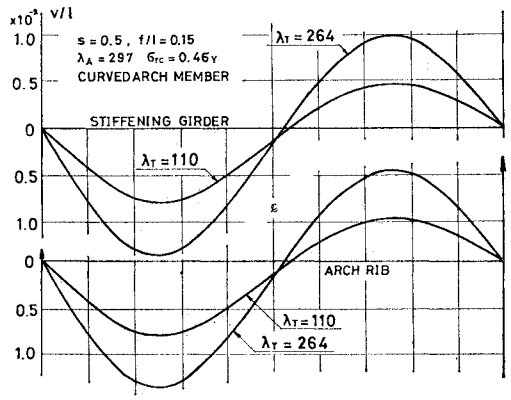

Fig. 4 Displacements of stiffening girders and arch ribs just before ultimate state for unsymmetrical loading.

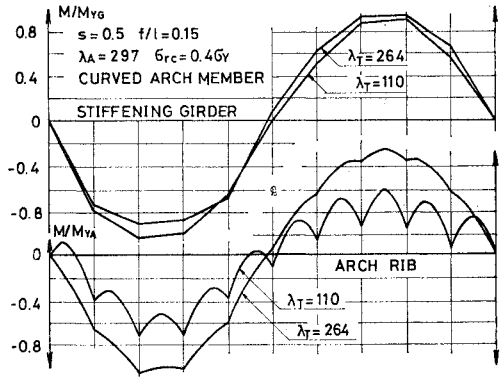

Fig. 5 Bending moment diagram of stiffening girders and arch ribs just before ultimate state for unsymmetrical loading.

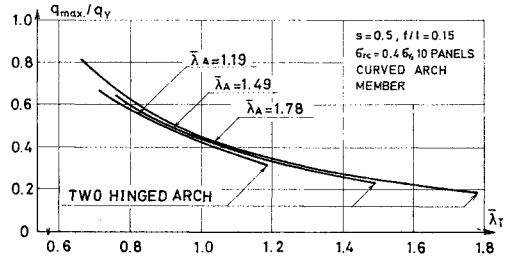

Fig. 6 Load carrying capacity of stiffened arches expressed by total slenderness parameter for unsymmetrical loading.

it shows always a little higher value than that of two hinged arches if compared by the total slenderness parameter. With increment of the flexural rigidity of stiffening girders against flexural rigidity of arches, the load carrying capacity increases also, but the efficiency of stiffening seems to be not so significant as illustrated in **Fig. 7**. But, by plotting the ratio of the maximum load to total area of arch rib and stiffening girder against the ratio of the flexural rigidity of arch rib to the total flexural rigidity, the efficiency of stiffening will be meaningly illustrated as seen in **Fig. 8**. The efficiency is generally improved by adopting more rigid stiffening girder. If the efficiency is compared on condition of the same maximum load, arches stiffened by a relatively rigid stiffening girder have always higher efficiency. In the calculated range, it is advisable to proportion more rigidity to the stiffening girder than the arch rib. But, by reasons which will be discussed in the following sections, the flexural rigidity required to arch ribs will be determined by the local behavior of the arch rib members.

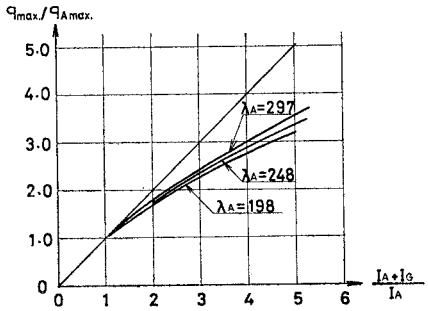

Fig. 7 Stiffening effect on the load carrying capacity for unsymmerical loadings.

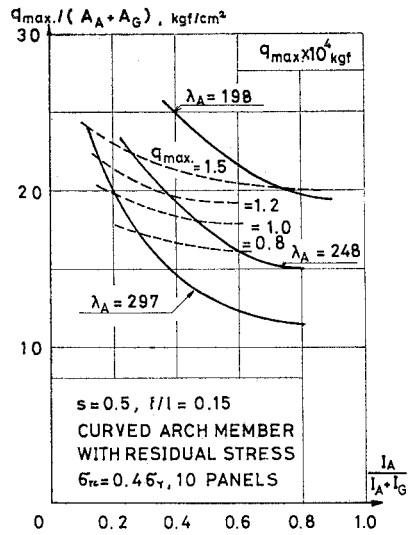

Fig. 8 Stiffening efficiency expressed by the ratio of the ultimate loads per total cross sectional area of stiffened arches to the ultimate loads per cross sectional area of the arch ribs.

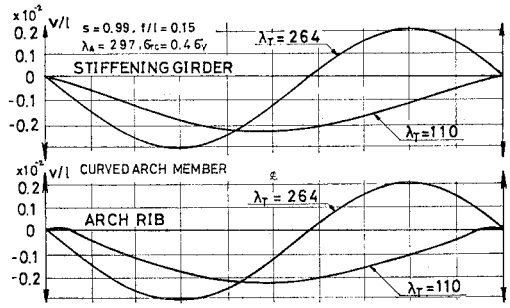

Fig. 9 Displacements of stiffening girders and arch ribs just before ultimate state for quasi-symmetrical loading.

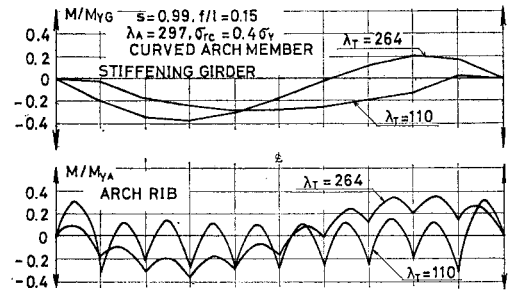

Fig. 10 Bending moment diagram of stiffening girders and arch ribs just before ultimate state for quasi-symmetrical loading.

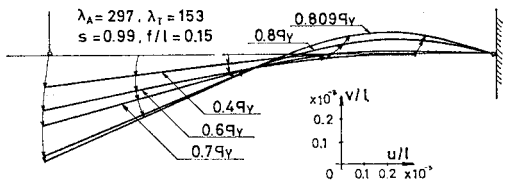

Fig. 11 Zoom up of the displacements of an end panel arch rib member for quasi-symmetrical loading.

(2) Behavior for Nearly Symmetrical Loading

Under the nearly symmetrical loading, the deflection curves in the nearly ultimate state differ in shape depending on the ratio of the total slenderness parameter to the slenderness parameter of arch ribs. An example is shown in **Fig. 9**. In the figure, the ordinate is expressed by the ratio of vertical deflection v to span length l. As to $\lambda_T=264$, i.e. arches with a relatively flexible stiffening girder, the collapse occurs in a nearly unsymmetrical mode, while in case of $\lambda_T=110$, i.e. arch with a relatively rigid stiffening girder, the collapse mode is rather symmetrical one. In both cases, the slenderness ratio of arch rib to be stiffened is not varied. This difference will be exhibited by the bending moment diagrams as shown in **Fig. 10**. In the former case, the highest bending moment of the arch rib is produced in the vicinity of the quater point, while, in the latter case, the bending moment becomes maximum at the end panels. **Fig. 11** illustrates the behavior of an end panel member. With the loads approaching to the ultimate value, the end panel member begins to show large upward deflection and the strength of the whole structure is governed by this local failure of the end panel member. This phenomenon is, of course, presented under the influence of the rather large crookedness of the continuously curved members and less end restraint at the hinged supports. The influence of this crookedness will be discussed in the section **3.(3), b)**.

(3) Load Carrying Capacity for Nearly Symmetrical Loading

a) Characteristics of Load Carrying Capacity

Fig. 12 shows the relationship between the load carrying capacity and the total slenderness parameter. In the range of higher slenderness parameter, these curves have a similar tendency with those obtained for the unsymmetry loadings as shown in **Fig. 6**, but always gives higher values than them. However, in the range of lower slenderness parameter, the curves become flat and hardly show increment of the load carrying capacity by the local failure of the arch rib members.

b) Influence of the Configuration of Arch Rib Members between Adjacent Panel Points

The crookedness of the arch rib members affects heavily their behavior in the ultimate state. **Fig. 13** shows the bending moment diagram just before the ultimate state of stiffened arches of which arch rib members have straight axis between the panel points. The significant undulation of bending moment which are produced in the continuously curved members as shown in **Fig. 5** diminishes due to the straightness of the members. The effect on the load carrying capacity is shown in **Fig. 14**, in which some cases of stiffened arches with very slender arch rib (λ_A= 446 and 595) are added. Note that the load carrying capacity in the range where the local failure is predominant is clearly improved by employment of the straight arch rib members.

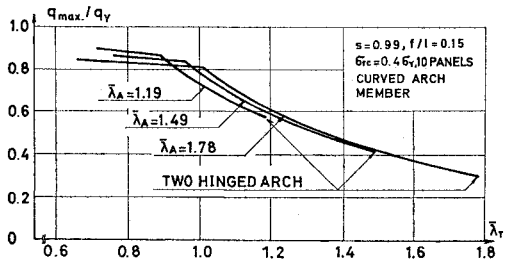

Fig. 12 Load carrying capacity of stiffened arches expressed by total slenderness parameter for quasi-symmetrical loading.

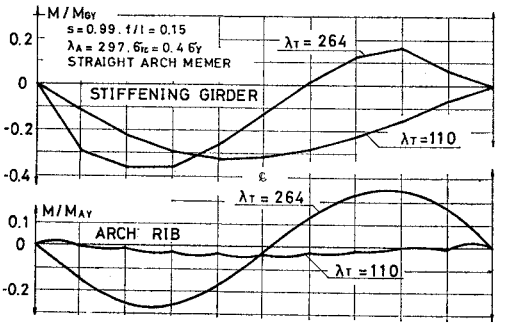

Fig. 13 Bending moment diagram of stiffened arch with straight arch rib members.

c) Influence of Initial Crookedness of Arch Rib Members

Straight members in actual structures have inherently initial crookedness, which affects always severely on the column strength. For example, by the column strength curves presented by Ref. 10), the effect is taken into account by estimating the initial crookedness of one-thousandth of the column length at the middle point. According to the commonly accepted value of the initial crookedness, and considering easy calculation, the initial crookedness of one-thousandth of the panel length at the middle point and the half sinusoidal form are adopted here. **Fig. 15** shows the effect of the initial crookedness on the load carrying capacity. In the case of the very slender arch rib members, the effect is clearly observed, but the effect is not so significant for the stiffened arches with a relatively rigid arch rib.

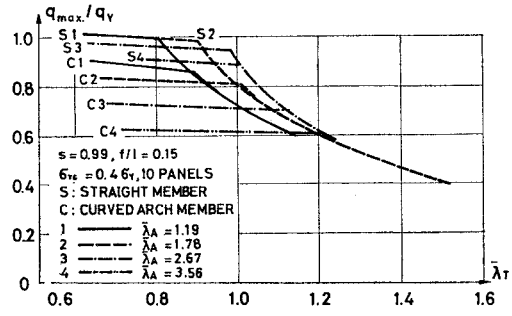

Fig. 14 Comparison between load carrying capacities of stiffened arches with straight arch rib members and curved ones.

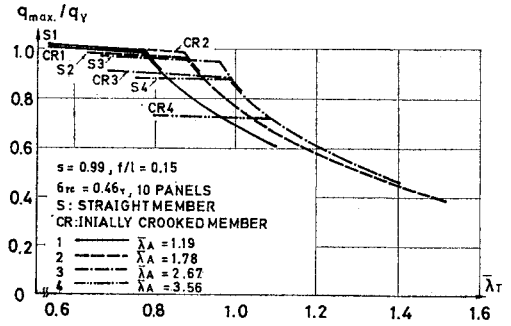

Fig. 15 Effect of initial crookedness of straight arch rib members on the local buckling strength.

d) Influence of Panel Length

As mentioned above, the number of panels of the standard stiffened arches analysed here is 10. With reduction of the number, the crookedness and the slenderness ratio of the members become larger. It causes reduction of the local failure strength.

Taking stiffened arches of 8 panels and $\lambda_A=198$ and 297 ($\bar{\lambda}_A=1.19$ and 1.78), this influence, in the cases of the continuously curved arch rib members and completely straight arch rib members, is shown in **Fig. 16**.

When the arch has completely straight rib members, this influence becomes fairly small even in the case of relatively high slenderness ratio. But, in the case of continuously curved rib members, the difference in the local failure strength becomes significant, especially for the more slender arch rib of $\lambda_A=297$.

As for the unsymmetrical loading, the influence of the panel length is negligibly small.

(4) Influence of Rise-Span Ratio

Fig. 17 shows the influence of rise-span ratio on the load carrying capacity as varying the ratio 0.125, 0.15 and 0.2. When the rise of stiffened arches becomes higher, the load carrying capacity decreases to some extent for the unsymmetrical loading and contrary to this tendency, increases slightly for the symmetrical loading. However, the local failure strength shows almost the same value, if expressed by the non-dimensional load intensity adopted here. In the calculated range, it is seen that the difference in the load carrying capacity between the high and low arches is not substantially large and has a similar tendency with that between two hinged arches.

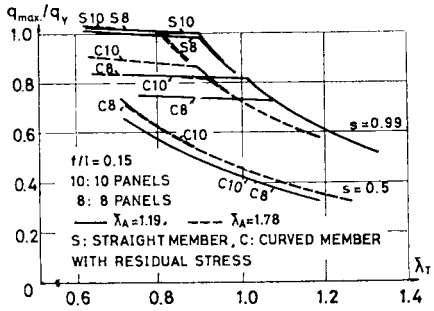

Fig. 16 Effects of panel length on the local buckling strength.

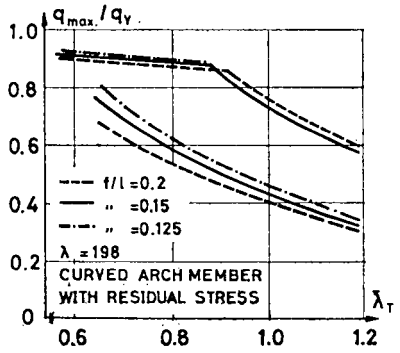

Fig. 18 Effects of rise-span ratio on the load carrying capacity.

(5) Influence of Residual Stresses

It is widely reported[10] that the working of the residual stresses caused by welding or cooling is substantial to the hinge-ended column strength, especially for columns of medium slenderness ratio. Stiffened arches are subjected to complicated interaction of bending moments and thrust as shown in **Fig. 5** and **Fig. 10**. Nevertheless, the residual stresses is considered to play a role also in the load carrying capacity of an integrated structure and the members. **Fig. 18** shows the influence of the residual stresses on the load carrying capacity. The load carrying capacity is affected a little in the case of the unsymmetrical loading, but, to some extend for the failure as a whole in the case of the nearly symmetrical loading. However it is remarkable that the local failure strength is affected very little by the residual stresses. It would be resulted from the complex interaction of the constrained bending moment and the bending moment due to the finite displacements.

(6) Influence of Loading Pattern

In the previous numerical analysis, the behavior of stiffened arches in the ultimate state for two typical loading patterns of $s=0.5$ and $s=0.99$ is discussed. The load carrying capacity varies with the loading pattern as shown in **Fig. 19**. Concerning to the failure as a whole structure, the load carrying capacity always decreases with the loading pattern becoming to more un-

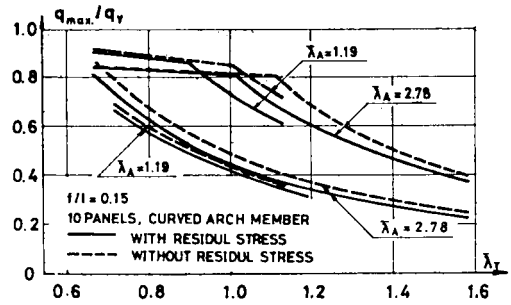

Fig. 17 Effects of residual stresses on the load carrying capacity.

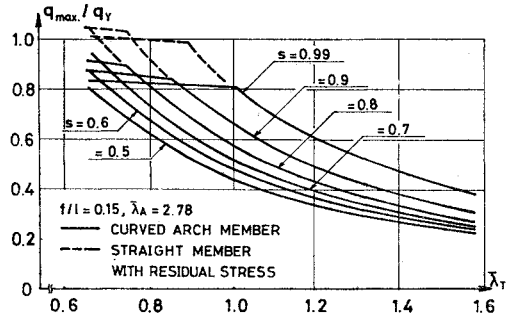

Fig. 19 Influence of loading pattern.

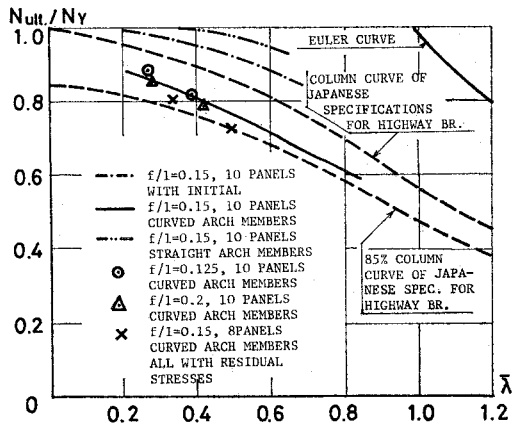

Fig. 20 Column strength curves for arch rib members of various type.

symmetrical as seen in the case of two-hinged arches[1),2)]. However, as to the local failure, decreasing of the load carrying capacity is found for more symmetrical loading pattern and this tendency may be valid for the case of other slenderness parameters, judging from the lower load carrying capacity for $s=0.5$ than for $s=0.99$ as shown in **Fig. 16, Fig. 17** and **Fig. 18**. This result leads to the conclusion that it is generally not required to pay attention to the local failure in the design of arch rib members for the unsymmetrical loading, if a check is made for their strength for uniformly distributed loads which are placed fully symmetrically over the entire span of arch or for the axial thrust caused by these loads. To establish a more exact practical rule for this problem, much additional numerical analysis will be required for arbitrary distributed loads. Excluding the local failure problem, the ultimate strength design of stiffened arch can follow that of two-hinged arches considering the similarity of the load carrying behavior of stiffened arches and two hinged arches.

(7) Local Failure Strength of Arch Rib Members

As discussed in the preceeding section, the local failure strength of arch rib members may be expressed by the maximum axial thrust which will be obtained at the end panels by the first order elastic analysis. Examined in detail, the local failure strength has a tendency to increase with increment of total slenderness ratio. Therefore, by estimating the smallest value in the nearly uniform strength region of the load carrying capacity curve for $s=0.99$ to be the ultimate strength of the member as a column, the column strength curves of the members is plotted in **Fig. 20** for all cases calculated here. In the figure, the basic column curve given by the Japanese specifications for highway bridges and a curve reduced by 15% are added. At least, in the calculated range of parameters, the strength of arch members for the local failure is not less than 85% of the basic column strength even in the case of continuously curved arch member. When straight or slightly initially crooked members are use, the strength are very improved and becomes larger than the basic column curve. This reduction of the strength in the case of the curved arch members would be the influence of the large crookedness of curved arch members. The strength of the end panel member shows always the smallest value among the members due to mainly the less end retraint at the hinged support and partly longest member length, if constant cross sections are used. Consequently, if a check is made for the strength of the end panel member, there will be no need of additional consideration on the local failure of the other members.

Judging from the figure, in the design of a stiffened arch with straight rib member, the member will be allowed to be proportioned according to the basic column curve. If continuously curved arch rib members are adopted, it is advisable to use the 85% curve as a tentative measure. Of course, wide range of calculation will be also required to determined the rational curve.

4. CONCLUSIONS

Through the numerical ultimate strength study which is carried out by considering the effects of geometrical and material nonlinearity and varying a certain number of structural parameters, the features of the in-plane load carrying capacity of stiffended steel arches were revealed fairly well. From the results obtained, the following conclusions may be led within the calculated range of treated parameters:

(1) The load carrying capacity of stiffened

arches has analogous features as that of two-hinged arches if they behave as an entirely integrated structure. The load carrying capacity shows always higher than that of two-hinged arches if compared by the total slenderness parameter.

(2) Under certain loading for arches with a stiffening girder of relatively large flexual rigidity, local failure of arch rib member occurs between adjacent panel points.

(3) The critical panel for local failure is end panels if the arch rib has constant cross section.

(4) With the loading pattern becoming more symmetrical, the ultimate strength as an integrated structure increases but the local failure strength decreases.

(5) The local failure strength is affected by the shape of member axis and panel length.

(6) Rise-span ratio does not affect significantly the load carrying capacity if the ratio is expressed in relation to the total slenderness parameter.

(7) The residual stresses do not affect significantly the load carrying capacity for unsymmetrical loading and local failure of curved arch members but have influence on the load carrying capacity for symmetrical loading to some extent.

(8) In the ultimate strength design of stiffened arches, it will be recommended that high rigidity is assigned to the stiffening girder as much as possible instead of the arch rib, of which rigidity should be proportioned to prevent the local failure.

(9) The local failure strength of arch rib members can be determined by the basic column strength curve given by the Japanese specifications for highway bridges when they have straight member axis between adjacents panel points. However, for the curved arch rib members, it is advisable to estimate the strength reducing by 15% off.

5. ACKNOWLEDGEMENT

Part of this work was supported by the Funds of Aid for Scientific Researches from the Ministry of Education.

Notations

A_A: Sectional area of an arch rib
A_G: Sectional area of a stiffening girder
I_A: Moment of inertia of an arch rib
I_G: Moment of inertia of a stiffening girder
f: Rise of an arch rib
L: Whole length of an arch rib
l: Span length
L': Length of an arch rib member between the panel points
l': Panel length
λ_T: Total slenderness ratio given by $L/\sqrt{(I_A+I_G)/A_A}$
$\bar{\lambda}_T$: Total slenderness parameter given by Eq. (6)
λ_A: Slenderness ratio of an arch rib
$\bar{\lambda}_A$: Slenderness parameter of an arch rib given by taking $I_G=0$ in Eq. (2) and Eq. (6).
λ: Slenderness ratio of arch rib member given by $L'/\sqrt{I_A/A_A}$
λ: Slenderness parameter of an arch rib member given by $\lambda\sqrt{\sigma_Y/E}/\pi$
q: Concentrated load placed on a panel point
s: Loading parameter
σ_Y: Yield point
σ_{ro}: Maximum compressive residual stress
q_{max}: Ultimate load for a stiffened arch
q_{Amax}: Ultimate load for an arch rib
N_{ult}: Ultimate axial force acting on an arch rib member, which is calculated by the first elastic analysis
N_Y: Yield axial force of an arch rib member
γ: Angle of an arch axis to the horizontal line at the springing
B_A: Width of cross section of an arch rib
H_A: Depth of cross section of an arch rib
B_G: Width of flange of a stiffening girder
M_A: Bending moment of an arch rib
M_G: Bending moment of a stiffening girder
M_{AY}: Yield bending moment of an arch rib
M_{GY}: Yield bending moment of a stiffening girder
v: Vertical displacement
u: Horizontal displacement

REFERENCES

1) Harries, H.: Traglasten stählerner Zweigelenk bogen mit ausgebreiteten Fliesszonen, Der Stahlbau, No. 6, p. 170 and No. 8, p. 248, 1970.
2) Kuranishi, S. and Lu, L.: Load Carrying Capacity of Two Hinged Steel Arch, Proc. of JSCE, No. 204, 1972.
3) Kuranishi, S.: Allowable Stress for Two-Hinged Steel Arch, Proc. of JSCE, No. 213, 1973.
4) Shinke, T. et al.: Analysis of In-Plane Elasto-Plastic Buckling and Load Carrying Capacity of Arches, Proc. of JSCE, No. 244, (in Japanese).
5) Shinke, T. et al.: Analysis and Experiment on In-Plane Load Carrying Capacity of Arches, Proc. of JSCE, No. 263, 1977 (in Japanese).
6) Zui, et al: Ultimate Strength Analysis of Arches with Stiffening Girder, Annual Meeting

of JSCE, 1977 (in Japanese).
7) Komatsu, S. and Shinke, T.: Practical Formulas for In-Plane Load Carrying Capacity of Arches, Proc. of JSCE, No. 267, 1977 (in Japanese).
8) Kuranishi, S. and Yabuki, T.: Some Numerical Estimation to Ultimate Strength of Two-Hinged Steel Arches, No. 287, 1979.
9) Stüssi, F.: Aktuelle baustatische Probleme der Konstrucktion praxis, Schweiz Bauzeitung, 1935.
10) Beer, H. and Schulz, G.: Die Traglast des planmäßig mitting gedrückten Stabs mit Inperfection, Teil 1, 2, 3, Sonderdruck as VDI-Z Bd. 111, Nr. 21, Nr. 23, Nr. 24. 1969.

(*Received May 15, 1979*)